Available online at www.sciencedirect.com

ScienceDirect

www.elsevier.com/locate/jes

JES JOURNAL OF ENVIRONMENTAL SCIENCES

www.jesc.ac.cn

Exploration of reaction rates of chlorine dioxide with tryptophan residue in oligopeptides and proteins

Yuexian Ge[1], *Yu Lei*[1], *Xin Lei*[1], *Wenhui Gan*[2], *Longfei Shu*[1], *Xin Yang*[1,*]

[1] *School of Environmental Science and Engineering, Guangdong Provincial Key Laboratory of Environmental Pollution Control and Remediation Technology, Sun Yat-sen University, Guangzhou 510275, China*

[2] *Graduate School at Shenzhen, Tsinghua University, Shenzhen 518055, China*

ARTICLE INFO

Article history:
Received 26 February 2020
Revised 31 March 2020
Accepted 31 March 2020
Available online 16 April 2020

Keywords:
Chlorine dioxide (ClO_2)
Tryptophan
Protein
Disinfection
Water treatment

ABSTRACT

Chlorine dioxide (ClO_2), an alternative disinfectant to chlorine, has a superior ability to inactivate microorganisms, in which protein damage has been considered as the main inactivation mechanism. However, the reactivity of ClO_2 with amino acid residues in oligopeptides and proteins remains poorly investigated. In this research, we studied the reaction rate constants of ClO_2 with tryptophan residues in five heptapeptides and four proteins using stopped-flow or competition kinetic method. Each heptapeptide and protein contain only one tryptophan residue and the reactivity of tryptophan residue with ClO_2 was lower than that of free tryptophan (3.88×10^4 $(mol/L)^{-1}sec^{-1}$ at pH 7.0). The neighboring amino acid residues affected the reaction rates through promoting inter-peptide aggregation, changing electron density, shifting pK_a values or inducing electron transfer via redox reactions. A single amino acid residue difference in oligopeptides can make the reaction rate constants differ by over 60% (e.g. 3.01×10^4 $(mol/L)^{-1}sec^{-1}$ for DDDWNDD and 1.85×10^4 $(mol/L)^{-1}sec^{-1}$ for DDDWDDD at pH 7.0 (D: aspartic acid, W: tryptophan, N: asparagine)). The reaction rates of tryptophan-containing oligopeptides were also highly pH-dependent with higher reactivity for deprotonated tryptophan than the neutral specie. Tryptophan residues in proteins spanned a 4-fold range reactivity toward ClO_2 (i.e. 0.84×10^4 $(mol/L)^{-1}sec^{-1}$ for ribonuclease T1 and 3.21×10^4 $(mol/L)^{-1}sec^{-1}$ for melittin at pH 7.0) with accessibility to the oxidant as the determinating factor. The local environment surrounding the tryptophan residue in proteins can also accelerate the reaction rates by increasing the electron density of the indole ring of tryptophan or inhibit the reaction rates by inducing electron transfer reactions. The results are of significance in advancing understanding of ClO_2 oxidative reactions with proteins and microbial inactivation mechanisms.

Introduction

Chlorine dioxide (ClO_2), an alternative disinfectant to chlorine, has been widely used in water treatment plants. ClO_2 has been reported as being used in 8.1% of water treatment plants in the United States and 32.8% of those in China (AWWA Water Quality Division, 2000; Zhang et al., 2016). In comparison to chlorine, the generation of toxic halogenated disinfection byproducts (DBPs) is greatly reduced through ClO_2 oxidation (Han et al., 2017; Kim et al., 2017; Zhong et al., 2019). Meanwhile, ClO_2 has a superior ability to inactivate bacteria (Huang et al., 1996), viruses (Huang et al.,

* Corresponding author.
E-mail address: yangx36@mail.sysu.edu.cn (X. Yang).

https://doi.org/10.1016/j.jes.2020.03.059
1001-0742/

1997), fungi (Wilson et al., 2005) and protists (Zuo et al., 2006) including *Cryptosporidium parvum* oocysts (Chauret et al., 2001; Murphy et al., 2014) and *Giardia intestinalis* cysts (Winiecka-Krusnell and Linder, 1998). In order to achieve a health-based target and prevent viral disease outbreaks, it is important to investigate the mechanisms of microorganism inactivation by ClO_2 so as to guide the more effective and extensive application of ClO_2 for disinfection.

Although ClO_2 can penetrate cell walls and destroy the internal structures of microorganisms including proteins and genomes, it is generally believed that protein damage is the dominant inactivation mechanism (Krista et al., 2012; Ogata, 2007), as ClO_2 reacts more readily with amino acids than with nucleotides (Ison et al., 2006; Sharma, 2012). A study of the inactivation of human rotavirus (HRV) by ClO_2 reported that denaturation of virus proteins was the dominant inactivation mechanism and that there was no genome damage when the HRV was completely inactivated (Xue et al., 2013). Roller found that when *Haemophilus influenzae* were exposed to ClO_2, total dehydrogenase enzymes and protein synthesis were completely inhibited while DNA-transforming activity was not affected (Roller et al., 1980). Moreover, it was found that three bacteriophages (MS2, fr and GA) could be completely inactivated by ClO_2 as a result of capsid protein degradation, which inhibited the attachment of virus to host cells, before detectable genome damage had accumulated (Hauchman et al., 1986; Noss et al., 1986; Sigstam et al., 2013). Setlow has also suggested that a major inactivation mechanism of *Bacillus subtilis* spores by ClO_2 was the damage to the proteins related to germination on the inner membrane (Setlow, 2006; Young and Setlow, 2003). Cho et al. (2010) studied the inactivation of *E. coli* and found that ClO_2 could penetrate into the cytoplasmic membrane and degrade the intracellular β-D-galactosidase in *E. coli* cells. Thus, understanding the reaction of ClO_2 with protein is of great significance for advancing understanding of microbial inactivation. It is also necessary for better control of waterborne microorganisms in drinking water.

From the aspect of the molecular level of proteins, ClO_2 is a selective oxidant that only reacts with 5 out of 20 natural amino acids, which are cysteine, tyrosine, tryptophan (Trp), histidine and proline. Specifically, cysteine, tyrosine and tryptophan have much faster reaction rate constants with ClO_2 (10^4–10^7 $(mol/L)^{-1}sec^{-1}$) than histidine and proline (~10^{-2} $(mol/L)^{-1}sec^{-1}$) at pH 7.0 (Ison et al., 2006; Stewart et al., 2008; Tan et al., 1987). Tryptophan residues have been reported to be critical targets in the reaction between ClO_2 and proteins, causing fragmentation and denaturation of proteins (Andrea et al., 2013; Ogata, 2007). For example, ClO_2 inactivation of influenza A virus is due to the oxidation of a tryptophan residue (W153) in haemagglutinin (Ogata, 2012), destroying its ability to bind with host cells. ClO_2 oxidation of free amino acids has been well studied, especially with tryptophan. The reaction rate constant of tryptophan with ClO_2 is relatively constant at pH 5.0–7.0 (3.4×10^4 $(mol/L)^{-1}sec^{-1}$ at pH 7.0), but it increases rapidly with pH increasing from 7.0 to 10.0 (Merenyi et al., 1988; Stewart et al., 2008). Two moles of ClO_2 are needed to oxidize one mole of tryptophan. ClO_2 first abstracts one electron from tryptophan to form a tryptophan radical cation ($Trp^{\bullet+}$, $pK_a = 4.3$), which then deprotonates to form a neutral tryptophan radical ($Trp^{\bullet}$). $Trp^{\bullet}$ is unstable and immediately reacts with a second mole of ClO_2 to generate N-formylkynurenine, kynurenine, 3-hydroxykynurenine and other products (Merenyi et al., 1988; Stewart et al., 2008). Despite the understanding of reactions between ClO_2 and free tryptophan, the reactivity of ClO_2 with tryptophan in peptides and proteins is rarely studied. As the damages of peptides or proteins are directly related with the microbial inactivation during ClO_2 disinfection, a better understanding of ClO_2 reactions with peptides or proteins would help in defining effective ClO_2 treatment and in optimizing strategies for disinfection.

The reactivity of an amino acid residue in a peptide or protein can be affected by its relative position and neighboring residues. The accessibility of an amino acid residue to the oxidant determines its oxidation rate (Jensen et al., 2012; Sharp et al., 2004). A study of f2 viral capsid found that cysteine residues may not be accessible for reactions with ClO_2 due to their buried positions, although cysteine reacts rapidly with ClO_2 (Noss et al., 1986). The reactivity of singlet oxygen with exposed histidine (H54) in glyceraldehyde-3-phosphate dehydrogenase was 4-fold higher than that with buried histidine (H108) (Lundeen and Kristopher, 2013). The reactivity of singlet oxygen with exposed tryptophan was also higher than the buried one in proteins (Jensen et al., 2012). Meanwhile, neighboring amino acid residues may change the reactivity by affecting the surrounding microenvironment. For example, $Trp^{\bullet+}$ can be converted back to tryptophan by some hydroquinones and phenols (Jovanovic et al., 1986, 1991), which will slow down the oxidation of tryptophan by ClO_2. Tyrosine, containing a phenol moiety, may also convert $Trp^{\bullet+}$ back to tryptophan (Egli and Janssen, 2018). Neighboring amino acid residues can also increase the reactivity of tryptophan residues to oxidant. During the reaction of singlet oxygen with a protein—*Bacillus licheniformis* subtilisin Carlsberg, asparagine residue was proposed to induce the transfer of electron density to the neighboring tryptophan residue, speeding up the oxidation of the tryptophan residue (Jensen et al., 2012). These previous findings provide evidence that the reaction rate of a given amino acid residue depends on the local environment of the amino acid in a protein. However, the reactivity of ClO_2 with amino acids in peptides and proteins is missing and their reaction rate constants have not yet been reported.

The objective of this study is to quantify the reactivity of ClO_2 with tryptophan residue in peptides and proteins. Among the five chlorine dioxide oxidizable amino acids, we focused primarily on tryptophan because of its high reaction rate constant with ClO_2, the well-studied reaction mechanisms with ClO_2, and its prevalence in diverse proteins (e.g. capsid proteins, membrane proteins, vital enzymes). Firstly, five heptapeptides were designed and reacted with ClO_2. Each heptapeptide contained only one tryptophan residue and six other unreactive amino acid residues, which represent aliphatic residues (alanine and asparagines), aromatic residues (phenylalanine), cationic residues (arginine) and anionic residues (aspartic acid). The aim was to understand how the properties of neighboring amino acid residues influence the oxidation of the tryptophan residue. Secondly, four proteins were chosen and reacted with ClO_2, each of which contained only one tryptophan residue that varied in location and exposure. The evaluation aimed to understand how the position of tryptophan residue as well as its microenvironment within a protein affected the reactivity toward ClO_2.

1. Materials and methods

1.1. Chemicals, heptapeptides and proteins

L-tryptophan (≥98%) and L-tyrosine (≥98%) were obtained from Sigma (USA). The heptapeptides were synthesized and purified by Qiangyao Biotechnology Ltd. (China). They were AAAWAAA (98.80%), FFFWFFF (92.90%), RRRWRRR (98.08%), DDDWDDD (94.05%) and DDDWNDD (98.20%) (A = alanine,

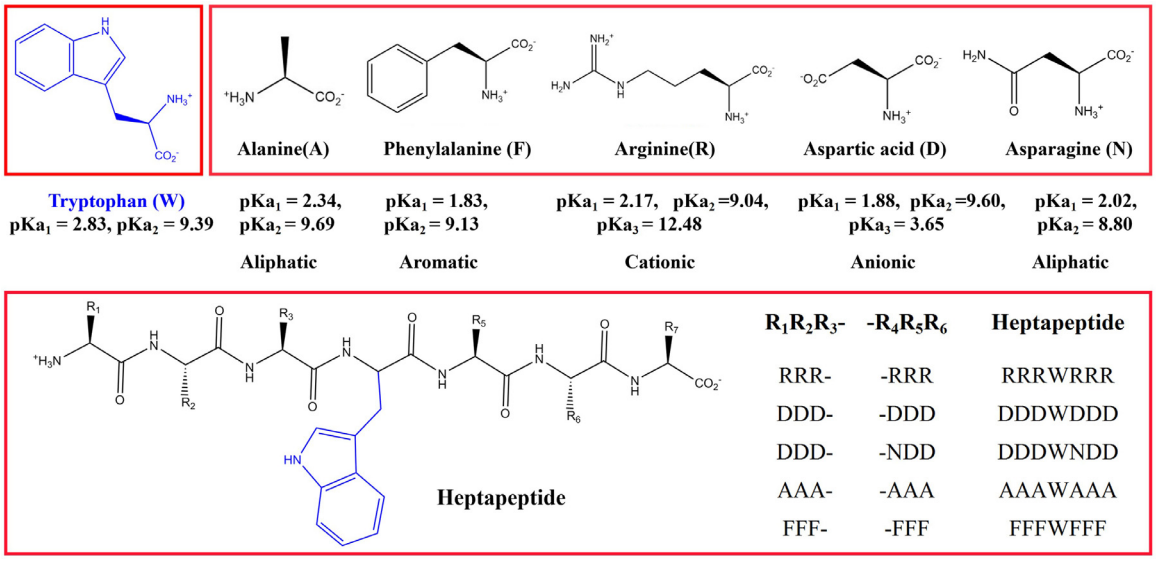

Fig. 1 – Structures of the heptapeptides and amino acids.

W = tryptophan, F = phenylalanine, R = arginine, D = aspartic acid, N = asparagine) (Fig. 1 and Appendix A Fig. S1). The presence of free tryptophan in the heptapeptides was negligible (<0.5%) (details in Appendix A Text S1). The four proteins evaluated were bee venom melittin (>85%, Sigma, USA), nuclease from *Staphylococcus aureus* (>40%, Sigma, USA), subtilisin Carlsberg from *Bascillus licheniformis* (150 U/mg, Sigma, USA) and ribonuclease T1 from *Aspergillus oryzae* (1 kU/μL, YuanYe, China). To prepare the stock solutions, tryptophan, DDDWDDD, DDDWNDD, RRRWRRR and the four proteins were dissolved directly in the buffered solutions. The AAAWAAA and FFFWFFF stock solutions were prepared by dissolving in 2% formic acid in water/methanol (50%/50%) solutions. The presence of 0.02% formic acid and 0.5% methanol in the diluted solution for reaction shall have little impacts on the determination of reaction rate constants of ClO_2 with tryptophan residue. Each of the heptapeptides and proteins contained only a single tryptophan residue. All the heptapeptides and proteins solutions were freshly prepared before use. Luminol (≥97%) was obtained from Sigma (USA) and dissolved in 0.01 M NaOH solution. The stock solution of ClO_2 was prepared from gaseous ClO_2 by slowly adding dilute H_2SO_4 to a sodium chlorite solution according to the standard method (APHA, 1998).

1.2. *Experimental procedures*

The reactions were conducted at pH ranging from 7.0 to 10.0. Samples were buffered with 10 mmol/L phosphate-buffered saline (PBS) solution for pH 7.0, 8.0 and 9.0 (137 mmol/L NaCl and 2.7 mmol/L KCl) or 10 mmol/L ammonia-ammonium buffered saline solution for pH 10.0 (137 mmol/L NaCl and 2.7 mmol/L KCl). The addition of NaCl and KCl was to maintain salt balance for the peptides and proteins. The reaction temperature was maintained at 25.0 (±1.0) °C using a circulating water bath monitored by a thermocouple (for stopped-flow kinetics measurements) or a constant temperature incubator (for competition kinetic measurements).

Reactions of ClO_2 with free tryptophan and RRRWRRR were investigated using stopped-flow decay kinetics method. The reactions were initiated by mixing excessive tryptophan or RRRWRRR (1–4 mmol/L) with 0.1 mmol/L ClO_2. A competition kinetic method was used to determine the reaction rate constants of ClO_2 with the heptapeptides (AAAWAAA, FFFWFFF, DDDWDDD and DDDWNDD) and proteins (Ren et al., 2018), as the reactions were quite fast and completed in a few minutes. Luminol was applied as the competitor. The reactions were conducted in 20 mL amber borosilicate bottles. The reactions were initiated by adding varying amounts of ClO_2 to buffered solutions containing 10 μmol/L luminol and 10 μmol/L heptapeptide or protein. Samples were taken until the ClO_2 had been completely consumed. The heptapeptide samples were analyzed using liquid chromatograph and the protein samples were analyzed using three-dimensional fluorescence spectrophotometry to track the changes of tryptophan residue concentration. The details for the calculation methods of the reaction rate constants of ClO_2 with the tryptophan residue in peptides and proteins were provided in Appendix A Text S2. The second-order rate constant of tyrosine's reaction with $Trp^{\bullet+}$ was measured using a laser flash photolysis technique (details in Appendix A Text S3) (Janssen et al., 2014; Lei et al., 2019). Duplicate or triplicate tests were performed, and the error ranges quoted for the rate constants are the 95% confidential intervals.

1.3. *Analytical methods*

The ClO_2 loss was tracked using its maximum absorbance at 360 nm ($\varepsilon = 966\ cm^{-1}(mol/L)^{-1}$) for the stopped-flow kinetics tests and its loss was tracked on a chlorine analyzer (DR2800, HACH, USA) based on diethyl-p-phenylene diamine (DPD) colorimetric method for the competition kinetics tests (APHA, 1998). The stopped-flow kinetics tests were performed using a stopped-flow spectrometer (SX20, Applied Photophysics, UK) equipped with a SX photodiode array detector.

Luminol, tryptophan, AAAWAAA, FFFWFFF, DDDWDDD and DDDWNDD concentrations were measured on a high-performance liquid chromatograph (U3000, Thermo Scientific, USA) equipped with a fluorescence detector and an Agilent ZORBAX SB-C_{18} column (4.6 mm × 250 mm, 5 μm particle size). The mobile phase for the determination of luminol, tryptophan, AAAWAAA, DDDWDDD and DDDWNDD was 25% acetonitrile and 75% 30 mmol/L sodium acetate buffer (pH 5.7). The mobile phase for the determination of FFFWFFF was 90% acetonitrile and 10% 30 mmol/L sodium acetate buffer (pH 5.7). The excitation and emission wavelengths for luminol detection were 380 nm and 425 nm, respectively and those

Table 1 – The second-order reaction rate constants of ClO_2 with tryptophan, luminol and tryptophan residues in heptapeptides.

Substance	k (10^4 (mol/L)$^{-1}$sec^{-1})			
	$k_{pH=7.0}$	$k_{pH=8.0}$	$k_{pH=9.0}$	$k_{pH=10.0}$
luminol (competitor)	7.10±0.17	8.82±0.14	16.5±0.24	26.8±0.26
tryptophan (W)	3.88±0.39	4.18±0.32	5.16±0.64	9.19±0.85
RRRWRRR	3.18±0.15	3.27±0.18	3.81±0.25	2.51±0.32
DDDWDDD	1.85±0.21	1.88±0.32	3.61±0.41	4.39±0.87
DDDWNDD	3.01±0.24	/	/	/
AAAWAAA	1.92±0.29	/	/	/
FFFWFFF	0.61±0.09	/	/	/

W = tryptophan, R = arginine, D = aspartic acid, N = asparagine, A = alanine, F = phenylalanine

for tryptophan or heptapeptides were 300 nm and 350 nm, respectively.

The elimination of luminol and tryptophan residues in the protein samples were tracked using a three-dimensional excitation-emission matrix (3D-EEM) fluorescence spectrophotometer (Aqualog UV-800-C, HORIBA, Japan). The excitation spectra were scanned from 200 to 500 nm in increments of 5 nm by varying the emission wavelength from 243 to 830 nm with 2.36 nm increments. Under the same conditions, the EEM spectrum of ultra-pure water was recorded as a blank and then subtracted from the EEM spectrum of each sample to eliminate water's Raman scattering and other background noise (Zhang et al., 2018). The excitation and emission wavelengths for quantifying luminol and tryptophan residues in proteins were the same as those in the high-performance liquid chromatography (HPLC) analyses.

The tryptophan-solvent accessible surface area (Trp-SASA) in the proteins were calculated from the static crystal structures using the GETAREA online facility (http://curie.utmb.edu/getarea.html) (Lundeen and Kristopher, 2013). GETAREA is an algorithm that computes the accessible surface areas of residues (relative to a certain probe radius) using atomic coordinates from crystal structure data. The PDB file identifiers for bee venom melittin, nuclease from *Staphylococcus aureus*, subtilisin Carlsberg from *Bacillus licheniformis* and ribonuclease T1 from *Aspergillus oryzae* were 6DST, 1F2M, 1BFU and 1FYS respectively. The default radius of the water probe (1.4 Å) on an area-per-residue basis was used. Software UCSF Chimera was used to determine distances between tryptophan residues and its neighboring amino acid residues according to crystal structures of the studied proteins (Pettersen et al., 2004). Quantum chemical calculations were performed using the GAUSSIAN 09 program package (details in Appendix A Text S4).

2. Results and discussion

2.1. *The reaction of ClO_2 with free tryptophan and tryptophan residue in heptapeptides*

Table 1 shows the reaction rate constants of ClO_2 with free tryptophan and tryptophan residue in heptapeptides (details in Appendix A Figs. S2 and S3). The second-order reaction rate constant of ClO_2 with free tryptophan was determined to be 3.88×10^4 (mol/L)$^{-1}$sec^{-1} at pH 7.0, being consistent with that reported from a previous study (3.4×10^4 (mol/L)$^{-1}$sec^{-1}) (Stewart et al., 2008). Luminol, the competitor for the competition kinetics study, reacted with ClO_2 at 7.1×10^4 (mol/L)$^{-1}$sec^{-1} at pH 7.0. Tryptophan residue in tested heptapeptides exhibited lower reaction rate constants than free tryptophan. Among these heptapeptides, tryptophan residue in RRRWRRR had the highest reaction rate constant with ClO_2 (3.18×10^4 (mol/L)$^{-1}$sec^{-1}) at pH 7.0, whereas tryptophan residue in FFFWFFF had the lowest reaction rate constant (0.61×10^4 (mol/L)$^{-1}$sec^{-1}). The reaction rates of tryptophan residues in DDDWDDD and AAAWAAA were very close at pH 7.0, which were 1.85×10^4 (mol/L)$^{-1}$sec^{-1} and 1.92×10^4 (mol/L)$^{-1}$sec^{-1}, respectively. Interestingly, although the amino acid sequences of DDDWDDD and DDDWNDD are very similar, the reaction rate of tryptophan residue in DDDWNDD (3.01×10^4 (mol/L)$^{-1}$sec^{-1}) was 62.7% higher than that in DDDWDDD (1.85×10^4 (mol/L)$^{-1}$sec^{-1}). The results suggested that neighboring amino acid residues greatly affected the reaction rate constants of tryptophan residues.

The properties of neighboring amino acids had great impacts on the accessibility of the tryptophan residue to ClO_2 by forming complex secondary structures. The primary structures of the heptapeptides are shown in Appendix A Fig. S1. Electrostatic interaction is the major interaction among the ionic polypeptides. Because of same-charge repulsion, RRRWRRR and DDDWDDD cannot form α-helix or β-sheet structures (Uversky, 2010) and they are in a stretched state in water, that is, random coil structure. FFFWFFF was the most hydrophobic heptapeptides among those studied, as phenylalanine was the most hydrophobic amino acid (Appendix A Table S1). Due to the hydrophobic driving force, FFFWFFF can fold spontaneously to form a β-folded structure. β-folded sheet structure also dominated in alanine (A) oligomers (Ma and Nussinov, 2010). Compared with coil structure, α-helix and β-sheet structures tend to have smaller water accessible surface area due to the presence of more hydrophobic amino acids (Garg, 2005). As such, the accessibility of tryptophan residues in DDDWDDD and RRRWRRR could have been higher than that in β-folded AAAWAAA and FFFWFFF, leading to higher reactivity of tryptophan residues in DDDWDDD and RRRWRRR. Besides intra-peptide aggregation, inter-peptide aggregation may also have occurred with the hydrophobic peptides in order to reduce the water contact area (Kim and Hecht, 2006). A previous study on the reactions of singlet oxygen reported that tryptophan residue in FFFHFFF in methanol reacted much more readily (5.4×10^7 (mol/L)$^{-1}$sec^{-1}) than in water (9.3×10^6 (mol/L)$^{-1}$sec^{-1}). It is therefore likely that intra-peptide and inter-peptide aggregation of FFFWFFF in water greatly reduced the accessibility of the tryptophan residue in FFFWFFF to ClO_2, resulting in the lowest reaction rate constant (0.61×10^4 (mol/L)$^{-1}$sec^{-1} at pH 7.0).

Moreover, electron-rich amide groups could induce electron transfer, increasing the reactivity of tryptophan residue. Besides tryptophan residue, DDDWDDD had six aspartic acid residues and DDDWNDD had five along with an asparagine residue. Unexpectedly, the reaction rate of tryptophan residue

in DDDWNDD (3.01×10^4 $(mol/L)^{-1}sec^{-1}$) was much higher than that in DDDWDDD (1.85×10^4 $(mol/L)^{-1}sec^{-1}$) at pH 7.0. Clearly, asparagine residue led to the increase in the reaction rate constants with ClO_2. ClO_2 is known to initially attack carbons 2 and 3 in the indole ring of tryptophan (Sharma, 2012; Stewart et al., 2008). According to Jensen's study, the electron-rich nitrogen and oxygen atoms of the amide group in asparagine residue may induce electron density on carbons 2 and 3 in the indole ring (Jensen et al., 2012), thus resulting in greater reactivity of tryptophan residue with ClO_2.

2.2. *Effect of pH on the reactivity*

The reaction rate constants showed pH-dependence based on the results of free tryptophan, DDDWDDD and RRRWRRR. As the pH increased from 7.0 to 10.0, the reaction rate constants of ClO_2 with free tryptophan increased from 3.88×10^4 to 9.19×10^4 $(mol/L)^{-1}sec^{-1}$. Similarly, ClO_2 oxidation rates of tryptophan residue in DDDWDDD more than doubled from pH 7.0 (1.85×10^4 $(mol/L)^{-1}sec^{-1}$) to pH 10.0 (4.39×10^4 $(mol/L)^{-1}sec^{-1}$). However, the reaction rate constants of ClO_2 with tryptophan residue in RRRWRRR showed little variation at pH 7.0–9.0 and decreased slightly at pH 10.0 (2.51×10^4 $(mol/L)^{-1}sec^{-1}$).

The pK_a values had great impact on the reaction rates. The pK_a values of the tryptophan residues in the heptapeptides were affected by the neighboring amino acids. The reaction rate constant of ClO_2 with free tryptophan increased sharply between pH 9.0–10.0 when the deprotonated ammonium group in tryptophan became dominant ($pK_a = 9.39$) (Appendix A Text S5, and Fig. 1). This was attributed to electrostatic interaction between the indole ring and the side chain. The indole ring was the site for ClO_2 attack, which initiated a single-electron abstraction reaction to form an indole cation radical (Sharma, 2012). When ClO_2 extracted an electron from tryptophan, the positive charge on the ammonium group close to the indole cation radical slowed down the reaction (Stewart et al., 2008). When the ammonium group was deprotonated, the reaction rates increased greatly as the electrostatic interaction was weakened. Over the tested pH range (7.0–10.0), DDDWDDD was negatively charged and RRRWRRR was positively charged. Electrostatic forces were assumed to be the major determinant of pK_a shifts of tryptophan residues in the peptides and proteins (Nielsen et al., 2011). No exact pK_a values were obtained for the tryptophan residues in heptapeptides, but the positively-charged guanidinium group of R may inhibit the protonation of tryptophan, leading to a lower pK_a. In contrast, the negatively-charged carboxylate groups of D may inhibit the deprotonation of tryptophan, leading to a higher pK_a. The shift in pK_a values of tryptophan residue in the heptapeptides thus affected the reactivity toward ClO_2 (Appendix A Fig. S4).

2.3. *The reaction of ClO_2 with tryptophan residue in the proteins*

In this study, four different proteins contained a single tryptophan residue were chosen: (1) Bee venom melittin (melittin), (2) nuclease from *Staphylococcus aureus* (nuclease), (3) subtilisin Carlsberg from *Bacillus licheniformis* (subtilisin Carlsberg), (4) ribonuclease T1 from *Aspergillus oryzae* (ribonuclease T1). Besides a tryptophan residue, nuclease and subtilisin Carlsberg contain 7 and 13 tyrosine residues, respectively. Ribonuclease T1 contains 9 tyrosine residues and 5 cysteine residues (Fig. 2). Based on the positions of the single tryptophan residue in the proteins tested, they were classified as exposed (in melittin), partially exposed (in nuclease and subtilisin Carlsberg) or buried (in ribonuclease T1) (Fig. 2). The classification is based on the relative accessible surface area (RASA)—the ratio between the SASA of the residue in proteins to that of its free state. The ranges of 0–10%, 10%-40%, and 40%-100% were used to define the status of buried, partially exposed and exposed, respectively (Nadericmanesh et al., 2001; Ma et al., 2015). The RASA values of melittin, nuclease, subtilisin Carlsberg and ribonuclease T1 were estimated as 75.2%, 19.8%, 21.2% and 0.5%, respectively (Appendix A Table S2), being consistent with the tryptophan exposure levels shown in Fig. 2.

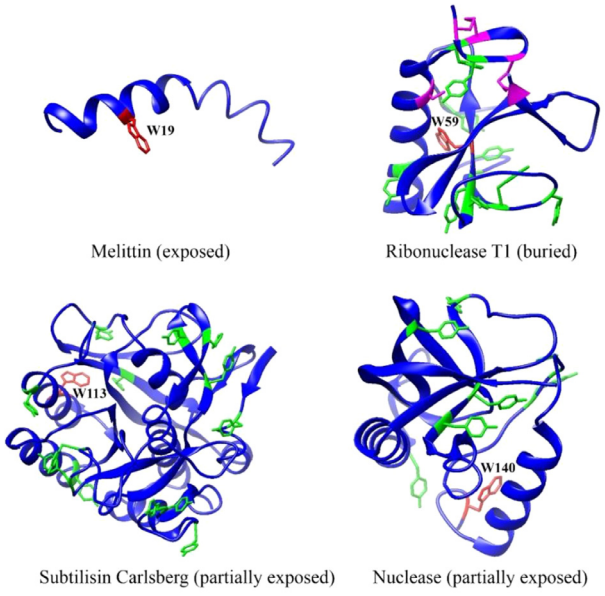

Fig. 2 – Three-dimensional structures of the four proteins. The single tryptophan residue is displayed in red, tyrosine residues are displayed in green, cysteine residues are displayed in pink.

The bleaching of tryptophan fluoresence was used to track the extent of ClO_2 oxidation of tryptophan residue in the proteins with luminol as the competing probe in the kinetics studies. Tryptophan fluorescence was tracked at 300 nm, an excitation wavelength at which the other amino acids would not be excited (Lakowicz, 2013). Luminol also absorbs at 300 nm, but luminol's fluorescence emission spectrum is different from that of tryptophan (Appendix A Fig. S5). Luminol fluorescence was tracked at 380 nm, an excitation wavelength at which tryptophan is not excited (Appendix A Fig. S5). Interference from the products generated was minimal (Daly et al., 2009; Eriksen et al., 1981; Sadowska Bartosz et al., 2014). We also checked the reaction rate constants of free tryptophan and luminol using both fluorescence analytical method and HPLC analytical method and found the difference was less than 20% (Appendix A Fig. S6). Thus, the decrease in tryptophan fluorescence can be reasonably used to reflect the changes in tryptophan concentration in the proteins.

The reaction rate constants for ClO_2 with tryptophan residue in the proteins are shown in Fig. 3. Tryptophan residue in melittin had the highest reaction rate constant with ClO_2 (3.21×10^4 $(mol/L)^{-1}sec^{-1}$) at pH 7.0, while tryptophan residue in ribonuclease T1 had the lowest (0.84×10^4 $(mol/L)^{-1}sec^{-1}$) (details in Appendix A Fig. S7 and Table S2). The reaction rates of tryptophan residue in subtilisin Carlsberg and nuclease were 2.77×10^4 $(mol/L)^{-1}sec^{-1}$ and 2.30×10^4 $(mol/L)^{-1}sec^{-1}$, respectively at pH 7.0. Note that tryptophan residue is well exposed in melittin and that it is buried in ribonuclease T1. In nuclease and subtilisin Carlsberg it is partially exposed.

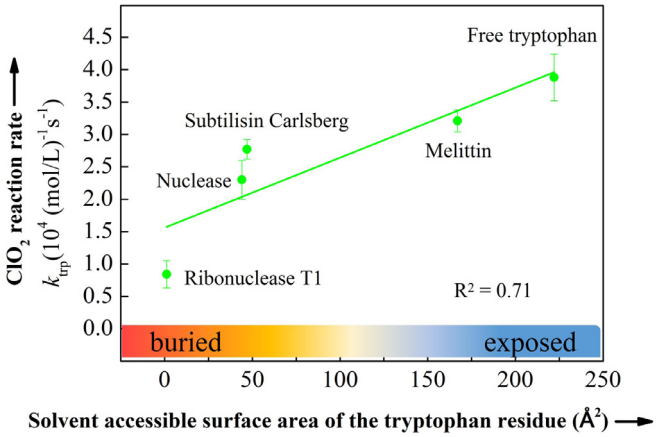

Fig. 3 – Specific reaction rate constants of ClO_2 with tryptophan residue in different proteins and with free tryptophan (k_{trp}) depending on the tryptophan-solvent accessible surface area (Trp-SASA). Trp-SASA indicates the accessibility of the tryptophan residue to solvent (ClO_2 solution), the greater the Trp-SASA value, the greater possibility the tryptophan residue is exposed to ClO_2.

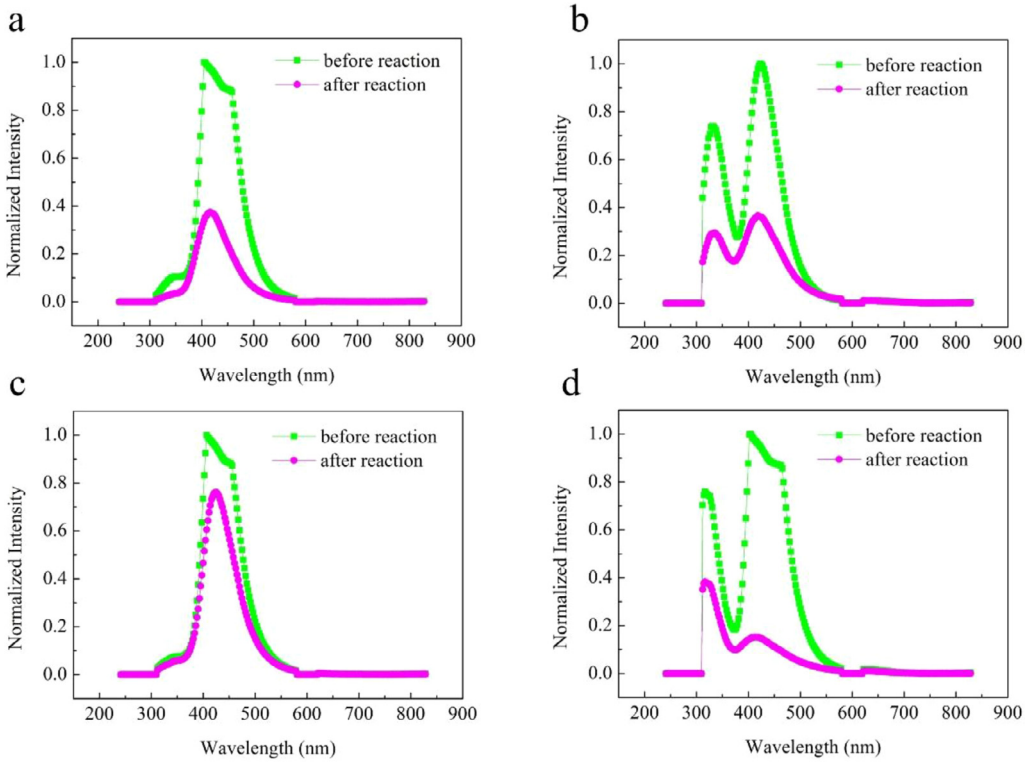

Fig. 4 – Fluorescence spectra of proteins before and after reaction with 36 μmol/L chlorine dioxide (a) Melittin; (b) Nuclease; (c) Subtilisin Carlsberg; (d) Ribonuclease T1. The excitation wavelength is 300 nm. The band whose λ_{max} falls in the range 310 to 350 nm is due to tryptophan emission. The band at $\lambda > 380$ nm is due to emission from the competitor, luminol.

To further validate the effect of accessibility of tryptophan residue, Trp-SASA was calculated. The greater the Trp-SASA value, the greater possibility that the tryptophan residue is exposed to ClO_2. The Trp-SASA values of melittin, nuclease, subtilisin Carlsberg and ribonuclease T1 were estimated as 167, 44, 47 and 1.1 Å^2, respectively (Appendix A Table S2), being consistent with the tryptophan exposure levels shown in Fig. 2. Fig. 3 relates the specific reaction rate constants of tryptophan residue in proteins with the Trp-SASA values. A modest correlation coefficient was observed ($R^2 = 0.71$), indicating that exposure level of the tryptophan residue in protein was an important factor affecting the reaction rates.

The local molecular microenvironment of the tryptophan residue in proteins may also have an effect, since two points in Fig. 3 deviate from the linear relationship. It is noteworthy that the intercept of the linear regression is not zero, meaning that buried residues can still react with ClO_2 to some extent. A reasonable explanation could be that Trp-SASA values were calculated from static crystal structure data, which may not

reflect the instantaneous accessibility of tryptophan residue as the protein moves about in solution (Richards, 1977). The reaction of ClO_2 with each protein was discussed in details below.

2.3.1. *Melittin*

The reaction rate of tryptophan residue in melittin with ClO_2 (3.21×10^4 $(mol/L)^{-1}sec^{-1}$) was 17.3% lower than that of free tryptophan (3.88×10^4 $(mol/L)^{-1}sec^{-1}$) at pH 7.0 although the tryptophan residue in this protein is well exposed. In fact, the estimated Trp-SASA value in melittin (167 $Å^2$) was lower than that of free tryptophan (222 $Å^2$) as a result of the α-helix structure. Moreover, melittin has a certain hydrophobic driving force, since 13 of its 26 amino acids are non-polar and hydrophobic (1 tryptophan, 2 alanine, 4 leucine, 3 isoleucine, 1 proline and 2 valine residues). It is therefore reasonable that the reaction rate of tryptophan residue in melittin would be slightly lower than that of free tryptophan.

2.3.2. *Nuclease*

The tryptophan residue in nuclease was classified as partially exposed with a Trp-SASA value (44 $Å^2$) much lower than that of melittin (167 $Å^2$). Compared with melittin, the spatial structure of nuclease is more complex. The secondary structure includes not only helices but also folded structures. The reaction rates of tryptophan residues in melittin and nuclease and that of free tryptophan were linearly related to their Trp-SASA values. Thus, the location of tryptophan residue seems to predominately determine its reaction rate with ClO_2 in nuclease.

2.3.3. *Subtilisin Carlsberg*

The tryptophan residue in subtilisin Carlsberg was also deemed partially exposed with a Trp-SASA value like that in nuclease. However, the reaction rate of tryptophan residue in subtilisin Carlsberg was 20.4% higher than that in nuclease. We examined the neighboring amino acids and found an asparagine residue close to the tryptophan residue (4.27 Å) (Fig. 4). We conducted quantum chemical calculations and found that the Mulliken charge and natural population analysis charge of the indole ring of tryptophan increased when there was a neighboring asparagine residue (Appendix A Text S4, and Table S4). Therefore, the amide group in asparagine (structure shown in Appendix A Fig. S8) could induce electron density on the indole ring of tryptophan, resulting in faster oxidation, as indicated by the study of the reactions of ClO_2 with DDDWDDD and DDDWNDD above.

2.3.4. *Ribonuclease T1*

Tryptophan residue in ribonuclease T1 was the least exposed and had the lowest reactivity among the four proteins. The deviation of reaction rate from the linear relationship (Fig. 3) indicated that there may be other factors slowing down the reaction. We examined the neighboring amino acids and found that there was a tyrosine residue near the tryptophan residue (10.57 Å) (Appendix A Fig. S9). Tryptophan radical cation ($Trp^{\bullet+}$) can be reduced back to tryptophan by phenolic compounds (Egli and Janssen, 2018). In this study, the reaction rate of $Trp^{\bullet+}$ with tyrosine was examined experimentally to be 1.53×10^7 $(mol/L)^{-1}sec^{-1}$ (details in Appendix A Text S3, and Fig. S10). However, the direct electron transfer can only occur when the distance between the electron accepting indole nitrogen in tryptophan and the donating phenol oxygen in tyrosine was within 5.64 Å (Egli and Janssen, 2018). We further examined the amino acids residues in ribonuclease T1 and there was a basic histidine near the phenol moiety of the tyrosine (4.39 Å) (Appendix A Fig. S9). Through electrostatic interaction and formation of the hydrogen bonds with structural water in the protein, the base group of the histidine can serve as an electron transfer station and promoted the intramolecular electron transfer when the distance of tyrosine and tryptophan residue was between 5.64 Å and 17.14 Å (Chen et al., 2009; Xiong et al., 2010). Therefore, electron transfer is supposed to occur between $Trp^{\bullet+}$ and tyrosine residue in the ribonuclease T1, making the observed reaction rates of tryptophan residue in ribonuclease T1 lower than the predicted one based on Fig. 3. Moreover, it should be noted that significant blue-shift of maximum of tryptophan fluorescence (λ_{max} = 316 nm) was observed in ribonuclease T1, in comparison to free tryptophan (λ_{max} = 350 nm) (Appendix A Table S2 and Fig. 4). This implies a more nonpolar and hydrophobic local environment in ribonuclease T1 than in free tryptophan (Vivian and Callis, 2001), which could adversely influence the reaction rate.

It should be noted that reaction rate constants obtained from this study refers to the reactivity of the specific tryptophan residue with ClO_2, not the whole protein. In the proteins, tyrosine and cysteine, the ClO_2 reactive amino acid residues, were also co-present (Fig. 2). Their SASA and RASA values calculated and listed in Appendix A Table S3. For example, although the tryptophan residue in Ribonuclease T1 had very low reaction rate with ClO_2, some of the tyrosine and cysteine residues having high RASA can also be the attack sites for ClO_2. In this study, we used five heptapeptides and four proteins as model compounds to investigate the effect of position as well as microenvironment on ClO_2 reactivity of tryptophan residues. The results indicate that it may be possible to make preliminary prediction of the susceptibilities of virus to disinfectants based on the compositions, structures and functions of viral proteins. By recognizing the positions of these three reactive amino acid residues (cysteine, tyrosine and tryptophan) in proteins and utilizing the relationships between the accessibility of the typical amino acid residue and ClO_2 reactivity (e.g. Fig. 3), we may obtain the reaction rates of each residue in the protein and find the "hotspots" for ClO_2 reaction. Future studies should focus on ClO_2 oxidation of proteins or enzymes with biological functions to further improve understanding the inactivation of virus and bacteria.

3. Conclusions

This study makes quantitative evaluation of the reactivity of ClO_2 with tryptophan residue in oligopeptides and proteins and improves understanding of the relationship between the structures of proteins and their reactivity toward the oxidant. The reaction rate depends on both the tryptophan residue's position in the peptide or protein—its accessibility, and the surrounding amino acid residues. The reaction rate constant of the tryptophan residue in protein is significantly affected by the extent of exposure to the oxidant. The microenvironment around the tryptophan residue also affects the reaction rates through shifting pK_a values, changing electron density, and inducing electron transfer via redox reactions. In fact, the tryptophan residues in the four tested proteins span a 4-fold range of reactivity toward ClO_2. Among these influencing factors, the accessibility to the oxidant determinates the reactivity. Therefore, to access the protein damage rates in disinfection process, it is of importance to make a quantitative understanding of how the accessibility to the oxidant affects the amino acids reactivity.

Acknowledgments

This work was supported by the National Key Research and Development Program of China (No. 2017YFE0133200), the National Natural Science Foundation of China (Nos. 21622706

and 21876210) and the Guangdong Provincial Science and Technology Planning Project (No. 2019A050503006).

Appendix A Supplementary materials

Supplementary material associated with this article can be found, in the online version, at doi:10.1016/j.jes.2020.03.059.

REFERENCES

Andrea, A., Camilo, L.A., Marcelo, K., Eduardo, L., Davies, M.J., Eduardo, S., 2013. Chemical modification of lysozyme, glucose 6-phosphate dehydrogenase, and bovine eye lens proteins induced by peroxyl radicals: role of oxidizable amino acid residues. Chem. Res. Toxicol. 26 (1), 67–77.

AWWA Water Quality Division, 2000. Committee report: Disinfection at large and medium-size systems. J. Am. Water Works Assoc. 92 (5), 32–43.

Chauret, C.P., Radziminski, C.Z., Lepuil, M., Creason, R., Andrews, R.C., 2001. Chlorine dioxide inactivation of Cryptosporidium parvum oocysts and bacterial spore indicators. Appl. Environ. Microbiol. 67 (7), 2993–3001.

Chen, X., Zhang, L., Zhang, L., Wang, J., Liu, H., Bu, Y., 2009. Proton-regulated electron transfers from tyrosine to tryptophan in proteins: through-bond mechanism versus long-range hopping mechanism. J. Phys. Chem. B 113 (52), 16681–16688.

Cho, M., Kim, J., Kim, J.Y., Yoon, J., Kim, J.H., 2010. Mechanisms of Escherichia coli inactivation by several disinfectants. Water Res. 44 (11), 3410–3418.

Daly, S., Bianchini, R., Polefka, T., Jumbelic, L., Jachowicz, J., 2009. Fluorescence and coloration of grey hair. Int. J. Cosmet. Sci. 31 (5), 347–359.

Egli, C.M., Janssen, E.M.L., 2018. Proteomics approach to trace site-specific damage in aquatic extracellular enzymes during photoinactivation. Environ. Sci. Technol. 52 (14), 7671–7679.

Eriksen, T.E., Lind, J., Merényi, G., 1981. Oxidation of luminol by chlorine dioxide. Formation of 5-aminophthalazine-1, 4-dione. J. Chem. Soc. Faraday Trans. 77 (9), 2125–2135 1.

Garg, A., Kaur, H., Raghava, G.P.S., 2005. Real value prediction of solvent accessibility in proteins using multiple sequence alignment and secondary structure. Proteins Struct. Funct. Bioinform. 61 (2), 318–324.

Han, J., Zhang, X., Liu, J., Zhu, X., Gong, T., 2017. Characterization of halogenated DBPs and identification of new DBPs trihalomethanols in chlorine dioxide treated drinking water with multiple extractions. J. Environ. Sci. 58, 83–92.

Hauchman, F.S., Noss, C.I., Olivieri, V.P., 1986. Chlorine dioxide reactivity with nucleic acids. Water Res. 20 (3), 357–361.

Huang, J., Ren, N., Wang, L., Ma, F., Juli, 1996. Disinfection effect of chlorine dioxide on bacteria in water. Water Res. 31 (3), 607–613.

Huang, J., Wang, L., Ren, N., Liu, X.L., Sun, R.F., Yang, G., 1997. Disinfection effect of chlorine dioxide on viruses, algae and animal planktons in water. Water Res. 31 (3), 455–460.

Ison, A., Odeh, I.N., Margerum, D.W., 2006. Kinetics and mechanisms of chlorine dioxide and chlorite oxidations of cysteine and glutathione. Inorg. Chem. 45 (21), 8768–8775.

Janssen, E.M.L., Erickson, P.R., McNeill, K., 2014. Dual roles of dissolved organic matter as sensitizer and quencher in the photooxidation of tryptophan. Environ. Sci. Technol. 48 (9), 4916–4924.

Jensen, R.L., Arnbjerg, J., Ogilby, P.R., 2012. Reaction of singlet oxygen with tryptophan in proteins: a pronounced effect of the local environment on the reaction rate. J. Am. Chem. Soc. 134 (23), 9820–9826.

Jovanovic, S.V., Harriman, A., Simic, M.G., 1986. Electron-transfer reactions of tryptophan and tyrosine derivatives. J. Phys. Chem. 90 (9), 1935–1939.

Jovanovic, S.V., Steenken, S., Simic, M.G., 1991. Kinetics and energetics of one-electron-transfer reactions involving tryptophan neutral and cation radicals. J. Phys. Chem. 95 (2), 684–687.

Kim, D., Ates, N., Bekaroglu, S.S.K., Selbes, M., Karanfil, T., 2017. Impact of combining chlorine dioxide and chlorine on DBP formation in simulated indoor swimming pools. J. Environ. Sci. 58, 155–162.

Kim, W., Hecht, M.H., 2006. Generic hydrophobic residues are sufficient to promote aggregation of the Alzheimer's Aβ42 peptide. Proc. Natl. Acad. Sci. 103 (43), 15824–15829.

Krista Rule, W., Pecson, B.M., Thérese, S., Franziska, B., Tamar, K., 2012. Virus inactivation mechanisms: impact of disinfectants on virus function and structural integrity. Environ. Sci. Technol. 46 (21), 12069–12078.

Lakowicz, J.R., 2013. Principles of Fluorescence Spectroscopy. Springer Science & Business Media.

Lei, Y., Cheng, S., Luo, N., Yang, X., An, T., 2019. Rate constants and mechanisms of the reactions of $Cl^{\bullet}$ and $Cl_2^{\bullet-}$ with trace organic contaminants. Environ. Sci. Technol. 53 (19), 11170–11182.

Lundeen, R.A., Kristopher, M.N., 2013. Reactivity differences of combined and free amino acids: quantifying the relationship between three-dimensional protein structure and singlet oxygen reaction rates. Environ. Sci. Technol. 47 (24), 14215–14223.

Ma, B., Nussinov, R., 2010. Molecular dynamics simulations of alanine rich beta-sheet oligomers: Insight into amyloid formation. Protein Sci. 11 (10), 2335–2350.

Ma, J., Wang, S., 2015. Acconpred: Predicting solvent accessibility and contact number simultaneously by a multitask learning framework under the conditional neural fields model. Biomed. Res. Int. 2015 (2015), 1–10.

Merenyi, G., Lind, J., Shen, X., 1988. Electron transfer from indoles, phenol, and sulfite (SO_3^{2-}) to chlorine dioxide (ClO_2). J. Phys. Chem. 92 (1), 134–137.

Murphy, J.L., Haas, C.N., Arrowood, M.J., Hlavsa, M.C., Beach, M.J., Hill, V.R., 2014. Efficacy of chlorine dioxide tablets on inactivation of Cryptosporidium oocysts. Environ. Sci. Technol. 48 (10), 5849–5856.

Nadericmanesh, H., Sadeghi, M., Arab, S., Movahedi, A.A., 2001. Prediction of protein surface accessibility with information theory. Proteins Struct. Funct. Bioinform. 42 (4), 452–459.

Nielsen, J.E., Gunner, M., García Moreno, E.B., 2011. The pK_a cooperative: A collaborative effort to advance structure-based calculations of pK_a values and electrostatic effects in proteins. Proteins Struct. Funct. Bioinform. 79 (12), 3249–3259.

Noss, C.I., Hauchman, F.S., Olivieri, V.P., 1986. Chlorine dioxide reactivity with proteins. Water Res. 20 (3), 351–356.

Ogata, N., 2007. Denaturation of protein by chlorine dioxide: oxidative modification of tryptophan and tyrosine residues. Biochemistry 46 (16), 4898–4911.

Ogata, N., 2012. Inactivation of influenza virus haemagglutinin by chlorine dioxide: oxidation of the conserved tryptophan 153 residue in the receptor-binding site. J. Gen. Virol. 93 (12), 2558–2563.

Pettersen, E.F., Goddard, T.D., Huang, C.C., Couch, G.S., Greenblatt, D.M., Meng, E.C., et al., 2004. . UCSF Chimera—a visualization system for exploratory research and analysis. J. Comput. Chem. 25 (13), 1605–1612.

Ren, Y., Wang, J., Grosselin, B., Daële, V., Mellouki, A., 2018. Kinetic and product studies of Cl atoms reactions with a series of branched ketones. J. Environ. Sci. 71, 271–282.

Richards, F.M., 1977. Areas, volumes, packing, and protein structure. Annu. Rev. Biophys. Bioeng. 6 (1), 151–176.

Roller, S.D., Olivieri, V.P., Kawata, K., 1980. Mode of bacterial inactivation by chlorine dioxide. Water Res. 14 (6), 635–641.

Sadowska Bartosz, I., Galiniak, S., Bartosz, G., 2014. Polyphenols protect against protein glycoxidation. Free Radical Biol. Med. 75, S47.

Setlow, P., 2006. Spores of Bacillus subtilis: their resistance to and killing by radiation, heat and chemicals. J. Appl. Microbiol. 101 (3), 514–525.

Sharma, V.K., 2012. Reactivity of chlorine dioxide with amino acids, peptides, and proteins. Environ. Chem. Lett. 10 (3), 255–264.

Sharp, J.S., Becker, J.M., Hettich, R.L., 2004. Analysis of protein solvent accessible surfaces by photochemical oxidation and mass spectrometry. Anal. Chem. 76 (3), 672–683.

Sigstam, T., Gannon, G., Cascella, M., Pecson, B.M., Wigginton, K.R., Kohn, T., 2013. Subtle differences in virus composition affect disinfection kinetics and mechanisms. Appl. Environ. Microbiol. 79 (11), 3455–3467.

Stewart, D.J., Napolitano, M.J., Bakhmutova-Albert, E.V., Margerum, D.W., 2008. Kinetics and mechanisms of chlorine dioxide oxidation of tryptophan. Inorg. Chem. 47 (5), 1639–1647.

Tan, H.K., Wheeler, W.B., Wei, C.I., 1987. Reaction of chlorine dioxide with amino acids and peptides: Kinetics and mutagenicity studies. Mutat. Res. Genet. Toxicol. 188 (4), 259–266.

Uversky, V.N., 2010. What does it mean to be natively unfolded? Eur. J. Biochem. 269 (1), 2–12.

Vivian, J.T., Callis, P.R., 2001. Mechanisms of tryptophan fluorescence shifts in proteins. Biophys. J. 80 (5), 2093–2109.

Wilson, S., Wu, C., Andriychuk, L., Martin, J., Brasel, T., Jumper, C., et al., 2005. . Effect of chlorine dioxide gas on fungi and mycotoxins associated with sick building syndrome. Appl. Environ. Microbiol. 71 (9), 5399–5403.

Winiecka-Krusnell, J., Linder, E., 1998. Cysticidal effect of chlorine dioxide on Giardia intestinalis cysts. Acta Trop. 70 (3), 369.

Xiong, P., Nocek, J.M., Vura-Weis, J., Lockard, J.V., Wasielewski, M.R., Hoffman, B.M., 2010. Faster interprotein electron transfer in a [myoglobin, b5] complex with a redesigned interface. Science 330 (6007), 1075–1078.

Xue, B., Jin, M., Yang, D., Guo, X., Chen, Z., Shen, Z., et al., 2013. . Effects of chlorine and chlorine dioxide on human rotavirus infectivity and genome stability. Water Res. 47 (10), 3329–3338.

Young, S., Setlow, P., 2003. Mechanisms of killing of Bacillus subtilis spores by hypochlorite and chlorine dioxide. J. Appl. Microbiol. 95 (1), 54–67.

Zhang, H., Jia, Y., Khanal, S.K., Lu, H., Fang, H., Zhao, Q., 2018. Understanding the role of extracellular polymeric substances on ciprofloxacin adsorption in aerobic sludge, anaerobic sludge, and sulfate-reducing bacteria sludge systems. Environ. Sci. Technol. 52 (11), 6476–6486.

Zhang, J., Zhang, X., Chen, J., Deng, C., Xu, N., Shi, W., et al., 2016. Highly selective luminescent sensing of xylene isomers by a water stable Zn-organic framework. Inorg. Chem. Commun. 69, 1–3.

Zhong, Y., Gan, W., Du, Y., Huang, H., Wu, Q., Xiang, Y., et al., 2019. Disinfection byproducts and their toxicity in wastewater effluents treated by the mixing oxidant of ClO_2/Cl_2. Water Res. 162, 471–481.

Zuo, J., Cui, F., Qu, B., Zhu, G., 2006. Removal effect on *Mesocyclops leukarti* and mutagenicity with chlorine dioxide. J. Environ. Sci. 18 (5), 891–896.